INTERNATIONAL JOURNAL OF AUTOMOTIVE AND MECHANICAL ENGINEERING
ISSN: 2229-8649 e-ISSN: 2180-1606
VOL. 20, ISSUE 3, 2023, 10559 – 10573
DOI: https://doi.org/10.15282/ijame.20.3.2023.01.0815

اونيۏرسيتي مليسيا ڤهڠ
UNIVERSITI MALAYSIA PAHANG

RESEARCH ARTICLE

Implementation of Evolutionary Algorithms to Parametric Identification of Gradient Flexible Plate Structure

A. Jamali[1,*], M.H. Hassan[1], R.Lidyana[1] and M.S Hadi[2]

[1]Department of Mechanical Engineering, Faculty of Engineering, Universiti Malaysia Sarawak, 94000 Sarawak, Malaysia
[2]Faculty of Mechanical Engineering, Universiti Teknologi MARA, 40450, Shah Alam, Selangor, Malaysia

ABSTRACT - This paper focused on modelling of a gradient flexible plate system utilizing an evolutionary algorithm, namely particle swarm optimization (PSO) and cuckoo search (CS) algorithm. A square aluminium plate experimental rig with a gradient of 30° and all edges clamped were designed and fabricated to acquire input-output vibration data experimentally. This input-output data was then applied in a system identification method, which used an evolutionary algorithm with a linear autoregressive with exogenous (ARX) model structure to generate a dynamic model of the system. The obtained results were then compared with the conventional method that is recursive least square (RLS). The developed models were evaluated based on the lowest mean square error (MSE), within the 95% confidence level of both auto and cross-correlation tests as well as high stability in the pole-zero diagram. Investigation of results indicates that both evolutionary algorithms provide lower MSE than RLS. It is demonstrated that intelligence algorithms, PSO and CS outperformed the conventional algorithm by 85% and 89%, respectively. However, in terms of the overall assessment, model order 4 by the CS algorithm was selected to be the ideal model in representing the dynamic modelling of the system since it had the lowest MSE value, which fell inside the 95% confidence threshold, indicating unbiasedness and stability.

ARTICLE HISTORY
Received : 13th July 2022
Revised : 24th Nov. 2022
Accepted : 02nd March 2023
Published : 09th Sept 2023

KEYWORDS
Cuckoo search,
Evolutionary algorithm,
Gradient flexible plate,
Particle swarm,
System identification,

1.0 INTRODUCTION

The superiority of flexible plate structures such as lightweight, lower maintenance, lower energy consumption, and faster response intrigues various engineering industries like solar panels, bridge decks, aircraft [1], and ship bodies [2] as well as conveyor systems [3]. Despite the numerous benefits that a flexible structure provides, it is easily affected by vibration due to the presence of disturbance forces. Thus, the unwanted vibration leads to plate structural fatigue and durability problems which affect the plate stability and performance. Subsequently compromising the safety of working environments [4].

Unwanted vibration must be reduced for the plate's performance to be maintained. Therefore, passive vibration control (PVC) has been proposed. PVC primarily involves modifying the dynamic characteristics of the structure by adding an absorber and damper to prevent excessive vibration on the plate. The increase in weight structure, however, limits PVC, as this technology cannot sustain low-frequency vibration on the flexible plate. Therefore, active vibration control (AVC) is consequently introduced. The AVC is a method of suppressing undesired vibration by interfering with the principal disturbance source. To create a successful AVC scheme, the system modeling must be realistic enough to replicate the actual dynamic characteristics of the structure [5].

Dynamic model identification by experimentation is an effective way to obtain dynamic modelling. The characteristics of a complex structure normally identified in the nonlinear system can be included in the dynamic model. Researchers have used the System Identification (SI) method to model systems that approximate physical system behavior under diverse operating situations. Based on the observed input-output data, this method is used to determine the accurate model of a dynamic system [6]. A decent model can be found by employing an appropriate estimation optimization approach. Nowadays, many researchers employ evolutionary algorithms (EA) in their optimization efforts to identify the optimum model because EA has been proven to be effective.

For instance, particle swarm optimization (PSO), which was inspired by the intelligent social behaviour of social organisms such as flocks of birds and schools of fish, has gained researchers' attention in various optimization problem-solving due to its fast convergence as well as fewer parameters that need tuning [7]. For a similar system in research, Khoooshechin et al. investigated the optimal parameters of flexible square cascade multicomponent isotopes. The outcome showed PSO optimization managed to increase the enrichment of each isotope at any concentration [8]. Besides, Negri et al. obtained the natural frequencies and mode shapes by using the simulational model updating method that utilized PSO optimization [9]. In [10], the researchers used an improved PSO algorithm with a two-stage optimization approach to efficiently accelerate particle swarm optimization (EAPSO) for estimating the localization and quantification of the damaged elements in plate structures. Meanwhile, Wang et al. utilized PSO optimization to calculate the optimum

*CORRESPONDING AUTHOR | A. Jamali | ✉ jannisa@unimas.my

combination of parameters of arc length for the curve interpolation method for interpolating the stress field of a wind tunnel flexible plate [11]. Besides, Julai et al. [12] optimized the control parameters using PSO for a flexible plate for vibration cancelation.

Another widely used EA in engineering applications is the Cuckoo search (CS) algorithm, which was inspired by the reproduction strategy of cuckoo birds. The ability to converge optimally in global search problems makes it extensively used by researchers for optimization issues [13]. For example, Chavan and Pawar employed the CS algorithm for optimization, maximization of density and minimization of cycle time on the cold chamber die-casting process [14]. In [15], Tran-Ngoc et al. utilized the CS algorithm by improving the weight and bias parameters of Artificial Neural Network (ANN) to minimize the differences between real and desired outputs on steel bridge beam-like structures [16]. Another study that uses CS as an optimization approach is in [17], where the optimum parameters for both the parametric estimation in modelling development and the PID controller's parameters for a single-link flexible manipulator are determined. Besides, [18] studied the optimization of the proportional-derivative (PD) based controller parameters by CS algorithm for the control scheme of a single-link flexible manipulator. Apart from that, Xu et al. investigated the vibration structural damage identification by using CS algorithm on detecting the local damages from the nonlinear objective function established by utilizing the natural frequencies and modal assurance criteria [19].

It can be concluded that PSO has fast convergence and use few parameters. Meanwhile, CS is very effective in solving global optimization, and it has single parameters to be adjusted. The advantages of PSO and CS highlighted hereby have prompted an investigation into their capabilities. Therefore, this study aims to use both PSO and CS algorithm with a system identification approach to model a flexible plate structure tilted at a gradient of 30°. The attained model is validated in terms of input/output mapping, Mean square error (MSE), correlation test, and pole-zero stability diagram. The outcome of the study would determine the suitability of the EA algorithm for a gradient flexible plate. This will serve as a starting point for further improvements to the algorithm.

2.0 EXPERIMENTAL SETUP

An experimental setup was conducted to acquire the input-output vibration data from a 30° gradient flexible plate structure. Firstly, the experimental rig of 30° gradient flexible plate structure was designed then fabricated. The input-output vibration data were acquired experimentally by integrating National Instruments (NI) data acquisition and instrumentation system. A square aluminium thin plate was used in the experiment with a dimension of 50 cm × 50 cm × 0.15 cm with a gradient of 30°. The edges of the experimental rig were fully clamped. The specification of the 30° gradient flexible plate used in this study were listed in Table 1.

Table 1. The specification of the experimental rig

Specification	Value
Dimension (length×width×thickness) and orientation	0.5×0.5×0.0015 m with 30° gradient
Number of sections	10×10
Density, ρ	2.71×10^{3} kg/m^3
Mass moment of inertia, I	5.19×10^{-11} kg.m^2
Modulus of elasticity, E	7.11×10^{10} N/m^3
Poisson's ratio, v	0.3

A magnetic shaker (S 50018) was placed on the excitation point of the experimental rig to generate the actuation force. The magnetic shaker was connected to a function generator (GFG-82155A) through a power amplifier (BAA 60) to create a sinusoidal actuation force. Two pieces of piezo-beam type accelerometer (PCB Piezotronics-353B33 and Kistler-8640A50) were attached at the observation and detection point, respectively to acquire the acceleration signal that represents the vibration of the 30° gradient plate structure. The sampling times were set to 0.003 s. The piezo-beam type accelerometers were connected to the NI data acquisition system (NI 9232 and NI 9263) mounted on the NI Compact-DAQ (portable NI cDAQ-9174) is connected to the personal computer. A personal computer equipped with a 10th Generation Intel® Core™ i3-10105 Processor, 16GB RAM, and MATLAB R2018A software were used to analyze the required signal obtained from the experiment. The experimental setup and integration system are shown in Figure 1 to Figure 3, respectively.

3.0 SYSTEM IDENTIFICATION

SI method was defined by developing the model of the system based on the input-output of experimental data [4]. SI steps consist of data acquisition, model structure selection, parameter estimation, and model evaluation. In this study, the model was developed using an autoregressive with exogenous input (ARX) and the model parameters were estimated using a conventional algorithm which is the RLS and PSO as well as CS algorithm.

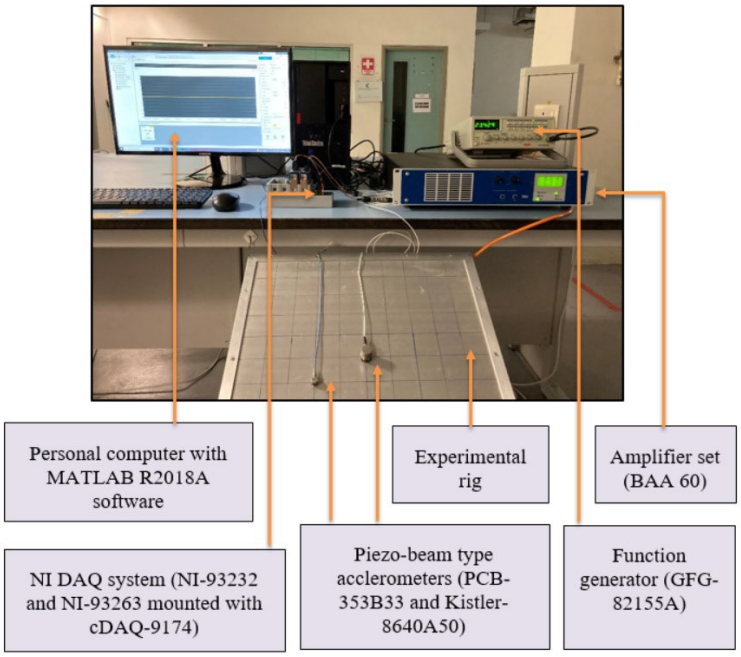

Figure 1. Experimental setup of 30° gradient flexible plate rig

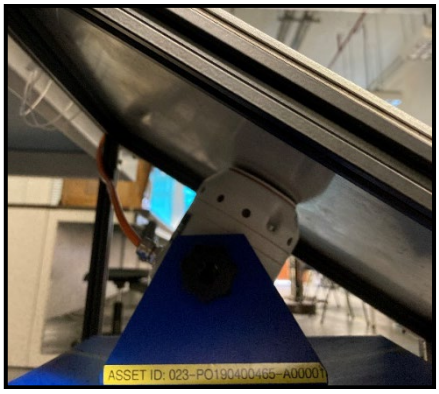

Figure 2. Location of magnetic shaker during experimental setup

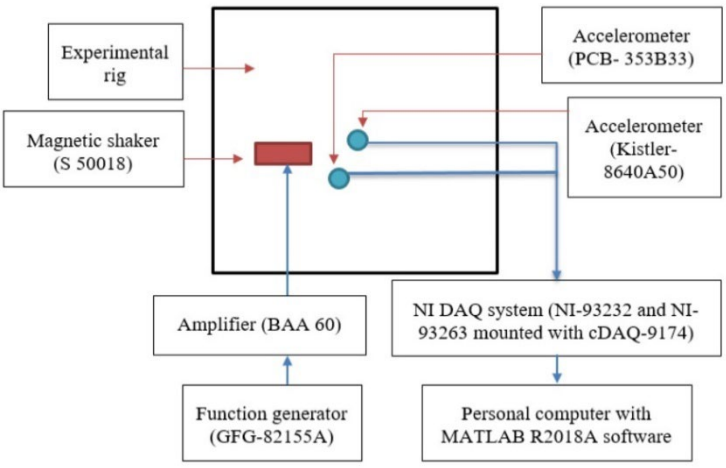

Figure 3. Schematic diagram of the flexible plate with 30° gradient setup

3.1 Data Acquisition

Data acquisition refers to the process of collecting data from various sources. In many cases, data acquisition involves processing data in real-time as it is collected, in order to ensure that the model being developed is accurate and can be used effectively. In this research, the experimental input-output data collection involves sensors, actuators, software, and other electronic components to collect data from the physical structure that is a flexible plate.

The magnetic shaker in the system provides an input signal. It produced an input acceleration signal to imitate the actual system under severe vibration. Accelerometer was placed on the detection point to measure this input signal. The

detection point is where the primary source of vibration or disturbance was detected. In order to detect the vibration output from the system, another accelerometer was employed to capture the acceleration signal which represents the vibration perceived by the gradient flexible plate. This was known as an observation point. The observation point is where the first mode of vibration occurred. The next three steps are explained in the following section.

3.2 Model Structure

A model structure is a transfer function that can represent the model of the system. In this study, the ARX model structure was selected due to the simplicity of its model structure in estimating the model parameters [6]. ARX model structure can be expressed as Eq. (1) and Eq. (2).

$$y(t) = \frac{B(z^{-1})}{A(z^{-1})}u(t) + \frac{1}{A(z^{-1})}\xi(t) \tag{1}$$

$$y(t) = -a_1 y(t-1) \dots -a_n y(t-n) + b_1 u(t-1) \dots b_n u(t-n) + \xi(t) \tag{2}$$

where *y(t)* is the output signal and *u(t)* is the input signal, respectively while $\xi(t)$ is the zero-mean white noise in the system. *n* is the order of the model while $a_1 \dots a_n$ and $b_1 \dots b_n$ were the parameters of the model.

3.3 Parameter Estimation

This study employs three types of algorithms for parameter estimation: RLS, PSO, and CS. The following is a detailed explanation of the algorithm.

3.3.1 Recursive least square

Recursive Least Square (RLS) algorithm is conventional parametric modelling based on a weighted least square criterion, used an iterative refinement technique to estimate the parameters continuously using previously existing parameters and information obtained from the continuous operation of the system [20]. In the RLS algorithm, the current parameter vector $\theta(i)$ is estimated based on the previous value of estimated vector $\theta(i-1)$. The accurate modelling can be determined by estimating the unknown parameters in real-time operation in this system.

$$\theta(i) = \theta(i-1) + K(i)E(i) \tag{3}$$

$$K(i) = \frac{\lambda^{-1}P(i-1)x(i)}{1 + \lambda^{-1}x(i)^T P(i-1)x(i)} \tag{4}$$

$$P(i) = \lambda^{-1}P(i-1) - \lambda^{-1}K(i)x(i)^T P(i-1) \tag{5}$$

$$E(i) = y(i) - x(i)^T \theta(i-1) \tag{7}$$

where $\theta(i)$ are the current parameter estimation and $\theta(i-1)$ is previous parameter estimation. λ is forgetting factor, x(i) is regression vector and y(t) is the output system.

3.3.2 Particle swarm optimization

Particle Swarm Optimization (PSO) introduced by Kennedy and Elberhart in 1995 is based on the social behaviour of social organisms such as a school of fish and a flock of birds which have great animal team behaviour. PSO algorithm is a stochastic and population-based swarm intelligence algorithm. PSO algorithm is widely known in research due to the advantages whereby PSO can be easily programmed with few parameters to control which makes the optimization process simpler. PSO also does not need prior knowledge of the problem-searching area [21].

Initially, the number of particles is randomly initialized and then flies through the space problem. The position of each particle was represented with *i*-th particle, represented in a *d*-dimensional vector in problem space as $X_i = (x_{i1}, x_{i2}, \dots, x_{id})$ where $i = 1, 2, \dots, n$ where *n* is defined as the number of particles. The velocity vector of *i*-th particle $v_i = (v_{i1}, v_{i2}, \dots, v_{id})$ was defined as the change of its position. Each particle memorizes the best position it has seen, thereby each particle's velocity and position are adjusted accordingly based on its memories. Meaning the particles always fly throughout the problem space to the best position. PSO algorithm completes the optimization after the personal best solution of each particle and global best values of the whole swarm were obtained. Every sample's error is calculated, and the mean squared error (MSE) is used as an objective function which is defined in Eq. (20). Thus, it is used to evaluate the algorithm's fitness score. The target is to reduce the fitness value and optimize the parameters.

The best fitness value is represented as $P_i (p_{i1}, p_{i2}, \dots, p_{id})$ while the fittest particle found at the time, *t* was represented as $P_g (p_{g1}, p_{g2}, \dots, p_{gd})$. Both velocities and positions of particles were updated based on the following equations:

$$v_{id}(t+1) = wv_{id}(t) + c_1 rand_1\left(p_{id} - x_{id}(t)\right) + c_2 rand_2\left(p_{id} - x_{id}(t)\right) \tag{8}$$

$$x_{id}(t+1) = x_{id}(t) + v_{id}(t+1) \tag{9}$$

where t is the number of iterations, c_1 and c_2 are acceleration coefficients, rand1 and rand2 are random numbers in the range [0, 1], and w is the inertia weight. The inertia weight, w is updated by the equation as shown below to reduce the weight over a number of iterations [7].

$$w = w_{max} - \left(\frac{w_{max} - w_{min}}{iter_{max}}\right)t \tag{10}$$

where w_{min} and w_{max} are the maximum and minimum values of inertia weight, while $iter_{max}$ is the maximum number of iterations. Figure 4 shows the flowchart of the PSO algorithm developed in this study.

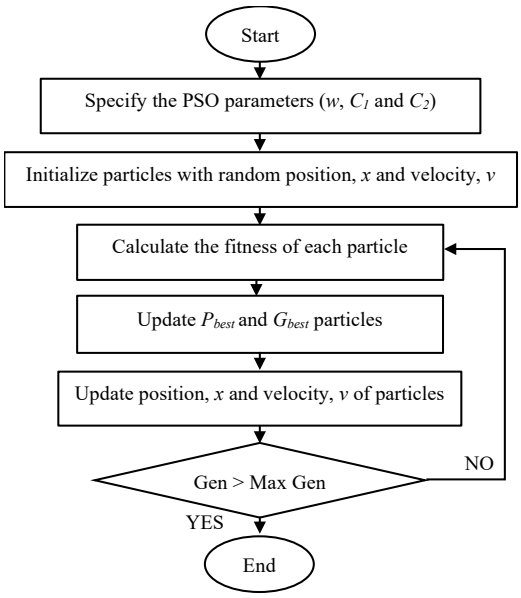

Figure 4. PSO algorithm flowchart

3.3.3 Cuckoo search algorithm

Inspired by brood parasitism reproduction of cuckoo birds, Cuckoo Search (CS) algorithms were introduced by Xin-She Yang and Suash Deb in 2009. Similar to the PSO algorithm, CS is also categorized as a stochastic and population-based swarm intelligence algorithm. The Cuckoo is considered a fascinating bird due to its aggressive reproduction strategy. Cuckoos lay eggs in communal nests and may remove other eggs to increase the hatching probability of their eggs. The ability of the CS algorithm to converge to global optimality is an advantage that is considered in the study. The switching or discovery probability in the CS algorithm controls both local search and global search capabilities [4, 12]. The switching probability affects the searching time of the local and global searches. A lower value of discovery rate will consequently increase the global search time and thus allow global optimality can be determined with a higher probability. The levy flight process that is used in the global search is another contributing factor to the CS algorithm. The levy flight process has infinite mean and variance, which allows the CS algorithm to explore the global search space more efficiently [12].

Initially, a population of host nests was initialized. The population was performed as follows:

$$x_{ij} = lb + rand_{ij}(ub - lb), i = 1, \dots, n; j = 1, \dots, mo \tag{11}$$

where x_{ij} is a solution that represents a cuckoo egg in a nest of the host while lb and ub represented the lower and upper boundary of the problem domain, respectively. $rand_{ij}$ is a random number from the uniform distribution within the interval, the range usually between 0 and 1. The exploration of search space was carried out by Levy flight process in cuckoo search is presented as:

$$x_i^{(t+1)} = x_i^t + \alpha S(x_i^t - x_{best}^t)r \tag{12}$$

where x_i^t is an individual current location, α is the step size variable, r is a random number resulting from the normal distribution and x_{best}^t is the current best nest, and S is a random walk based on Levy flights. The step length S is calculated using the Mantegna algorithm as shown in the following:

$$S = \frac{u}{|v|^{1/\beta'}} \tag{13}$$

where β is a parameter from range 1 to 2. The value of u and v can be obtained from normal distribution as follows:

$$\sigma_u = \left\{ \frac{\Gamma(1+\beta)\sin\left(\frac{\pi\beta}{2}\right)}{\Gamma\left[1+\frac{\beta}{2}\right]\beta 2^{(\beta-1)/2}} \right\}^{\frac{1}{\beta}}, \sigma_v = 1 \tag{14}$$

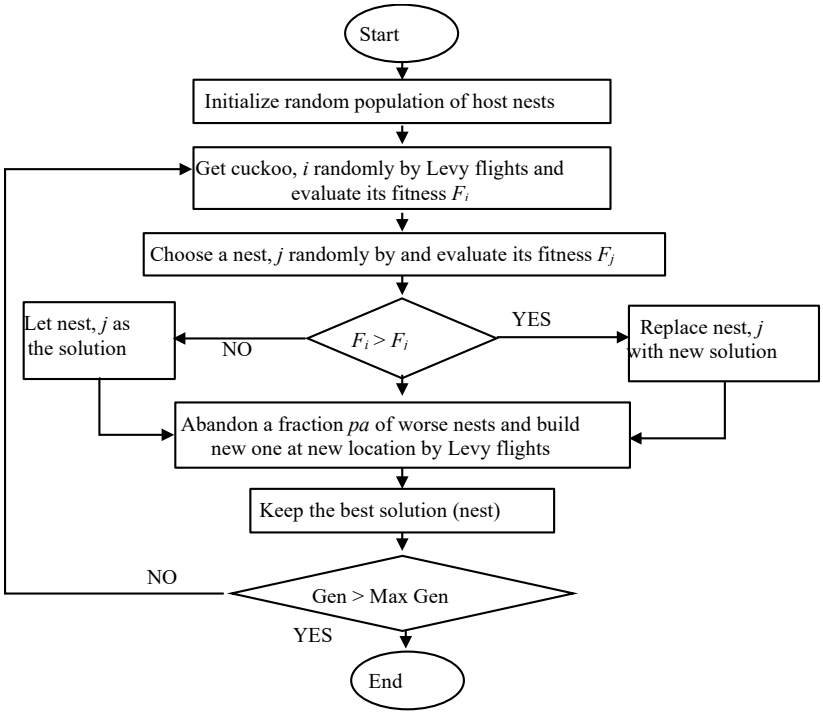

Figure 5. CS algorithm flowchart

3.4 Model Validation

Model validation is the last step in the system identification procedure. Validation of the developed model is very crucial to verify the optimum model, which represents the dynamic system of the 30° gradient flexible plate accurately. Four validation tests were considered for this study, namely one step ahead prediction (OSA), mean squared error (MSE), correlation tests, and pole-zero diagram stability. Al-Khafaji stated that the principles of model validation were comparing the actual and predicted output in time and frequency domain, respectively, as well as conducting the correlation test between input data and the prediction errors.

3.4.1 One step ahead prediction

One-step ahead prediction (OSA) is commonly used in model validation. The equation of OSA can be expressed as [19]:

$$\boldsymbol{y\hat{}(t) = f\left((u(t), u(t-1), \ldots, u(t-n_u, y(t), y(t-1), \ldots, y(t-n_y)\right)} \tag{18}$$

where *f(.)* is a nonlinear function while u and y are input and output, respectively. The equation of prediction error can be expressed as:

$$\boldsymbol{e(t) = y(t) - \hat{y}(t)} \tag{19}$$

where *e(t)* is the predicted error at time *t, y(t)* is the output system at time *t,* and *ŷ(t)* is one step ahead prediction model output at time *t*. If the value of residual is small, then the developed model meets the criteria, which can be validated by determining the residual between measured output and predicted output.

3.4.2 Mean squared error

In model validations, the mean squared error (MSE) is the most widely utilized besides OSA. The MSE is the difference between the actual output *y(n)* and the predicted output *ŷ(n)*. It can be expressed as [19]:

$$\boldsymbol{MSE = \frac{1}{N}\sum_{t}^{N}(y(t) - \hat{y}(t))^2} \tag{20}$$

where *y(n)* is the actual output attained from data acquisition, *ŷ(n)* is the predicted output produced from the optimization process via simulation and *N* is the number of input or output samples. The model meets the satisfied criteria if only the MSE value is small.

3.4.3 Correlation test

A correlation test is a statistical test representing the degree of relationship between two variables. Two types of correlation tests, namely autocorrelation and cross-correlation, are represented as vectors and matrices. The prediction of different data sets produced is accepted if the model was unbiased. Moreover, the prediction error is uncorrelated with all linear and nonlinear inputs and outputs if the model structure and estimated parameters are correct [21].

Autocorrelation's main purpose is to verify whether the error is independent of the past error. The equation of autocorrelation can be expressed as [22]:

$$\emptyset_{ee}(\boldsymbol{\tau}) = \boldsymbol{E}[\boldsymbol{e}(\boldsymbol{t}-\boldsymbol{\tau})\boldsymbol{e}(\boldsymbol{t})] = \boldsymbol{\delta}(\boldsymbol{t}) \tag{21}$$

where $\emptyset_{ee}(\tau)$ is the autocorrelation between $e(t)$ and $e(t-\tau)$, while $e(t)$ is the residual whereas $\delta(t)$ is an impulse function. The estimated autocorrelation should be zero when τ is non-zero, as the residual is white noise. The error is correlated where the model structure is unallocated when τ is non-zero. The autocorrelation test was considerably accepted if the correlation test achieved was within 95% of the confidence level and defined as $1.96\sqrt{N}$, where *N* is the length of data. Cross-correlation's main purpose is to verify whether the error is independent of the input signal. The equation of the cross-correlation test can be expressed as [19]:

$$\emptyset_{ue}(\boldsymbol{\tau}) = \boldsymbol{E}[\boldsymbol{u}(\boldsymbol{t}-\boldsymbol{\tau})\boldsymbol{e}(\boldsymbol{t})] = \boldsymbol{0} \ldots \forall \boldsymbol{\tau} \tag{22}$$

$\emptyset_{\mathrm{ue}}(\tau)$ is the cross-correlation between *u(t)* and *e(t)* which represent the input and residual, respectively. The residual is correlated with input when cross-correlation is non-zero for all τ. Similar to the autocorrelation test, cross-correlation test can be accepted if the correlation tests are achieved within 95% of the confidence level.

4.0 RESULTS AND DISCUSSION

In this study, a total of 4000 datasets were collected throughout the experimental test and the sampling time was set to 0.003 s. A total of 2000 data points were used for training, while the remaining 2000 points were used for testing.The optimum model should have the lowest MSE, the highest stability in the pole-zero diagram, and be within 95 percent confidence for both auto and cross-correlation tests.

4.1 Modelling using Recursive Least Square

The optimum model based on the RLS algorithm was fine-tuned by varying the model order and forgetting factor. Table 2 shows the initial RLS parameters. Model order 6 was shown to be the optimum, with the lowest mean square error of 6.645310^{-4} and 7.416210^{-5} for training and testing data, respectively. Figures 6 and 7 represent the actual and expected outputs of the 30° gradient flexible plate system in the time and frequency domains. Based on Figures 6 and 7, it was demonstrated that the developed model was capable of reproducing the actual result. It was supported by the relatively small error that occurred between the real and estimated outputs based on RLS modelling as shown in Figure 8.

Table 2. Parameter of optimum model for RLS modelling

Parameter	Value
Forgetting factor, λ	0.7
Model order	6
MSE for training data	6.6453×10^{-4}
MSE for testing data	7.4162×10^{-5}

Figures 9 and 10 show the pole-zero diagram and the correlation test, respectively. According to the pole-zero diagram, the RLS algorithm produced model was stable because all of the transfer function poles were inside the unity circle – (0,0) being the most stable. The efficiency of the RLS algorithm-developed model was tested using autocorrelation and cross-correlation tests. Based on both correlation tests, the RLS-developed model was found to be biased because the autocorrelation does not satisfy the 95 percent confidence level. Equation (23) expresses the transfer function of a 30° gradient flexible plate system based on RLS modelling.

$$\boldsymbol{H(z)_{RLS}} = \frac{-\boldsymbol{0.2925z^{-1} - 0.07901z^{-2} + 0.1838z^{-3} + 0.1676z^{-4} + 0.2917z^{-5} + 0.6337z^{-6}}}{\boldsymbol{1 + 0.08501z^{-1} + 0.1072^{-2} - 0.06673z^{-3} + 0.01804z^{-4} + 0.134z^{-5} - 0.361z^{-6}}} \tag{23}$$

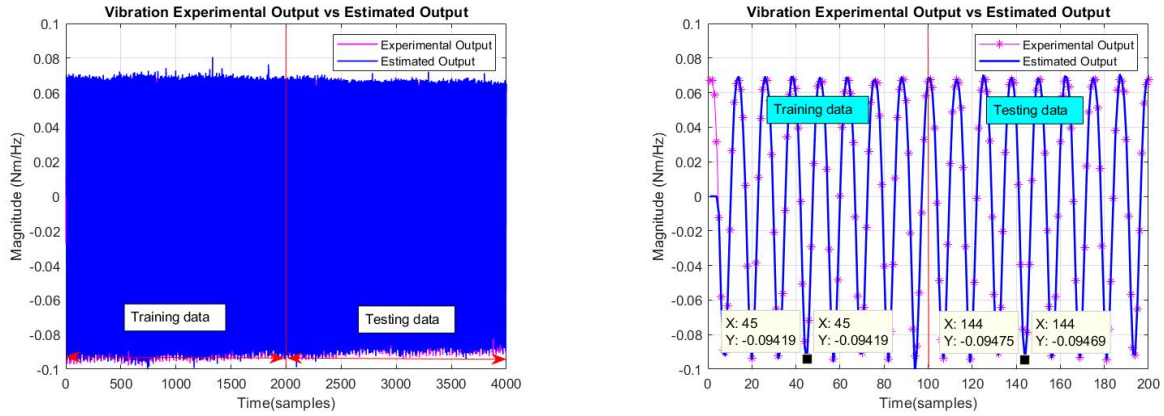

(a) (b)

Figure 6. Actual and prediction outputs of the system by RLS modelling in the time domain (a) estimated output for 4000 sample datasets and (b) an enlarged view of 200 sample datasets

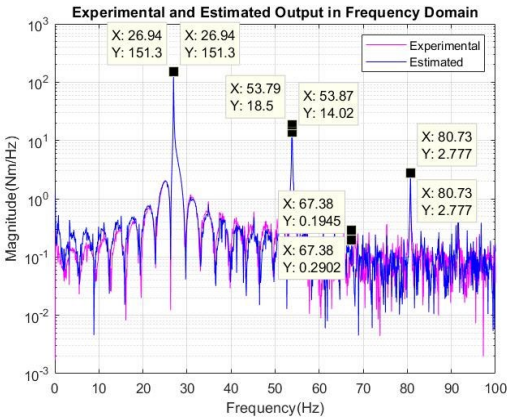

Figure 7. Actual and prediction outputs of the system by RLS modelling in the frequency domain

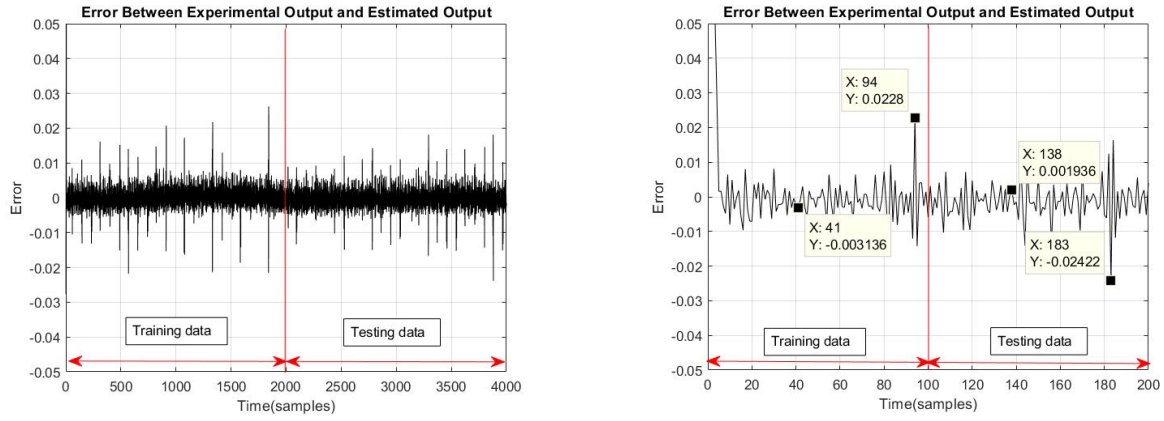

(a) (b)

Figure 8. Error between actual and estimated output by RLS modelling (a) sample for 4000 datasets and (b) an enlarged view of 200 datasets

The results show that the developed mathematical model of the gradient flexible plate, represented by the transfer function expressed in Eq. (23), generates a small mean square error (MSE) value when a model order of 6 is used. This suggests that this mathematical model can generate data that is closely aligned with the original data. In addition, the pole-zero diagram result indicates that the model is stable. System stability is a crucial performance specification for a control system that cannot be disregarded. Besides, although the correlation test was found to be biased, the model can still be accepted as this biasness indicates that the model is specialized for certain settings or universally applicable. Thus, it can be concluded that the developed mathematical model by using RLS can be used to represent the physical structure of the titled flexible plate.

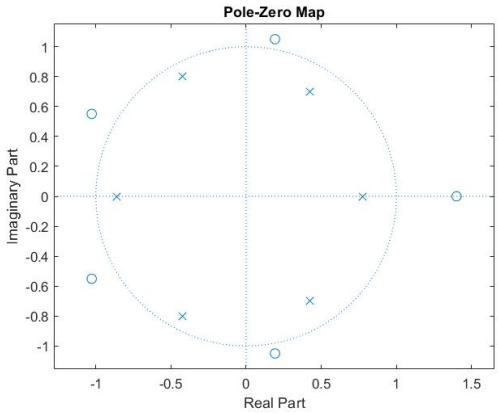

Figure 9. Pole-zero diagram system of model order 6 by RLS modelling

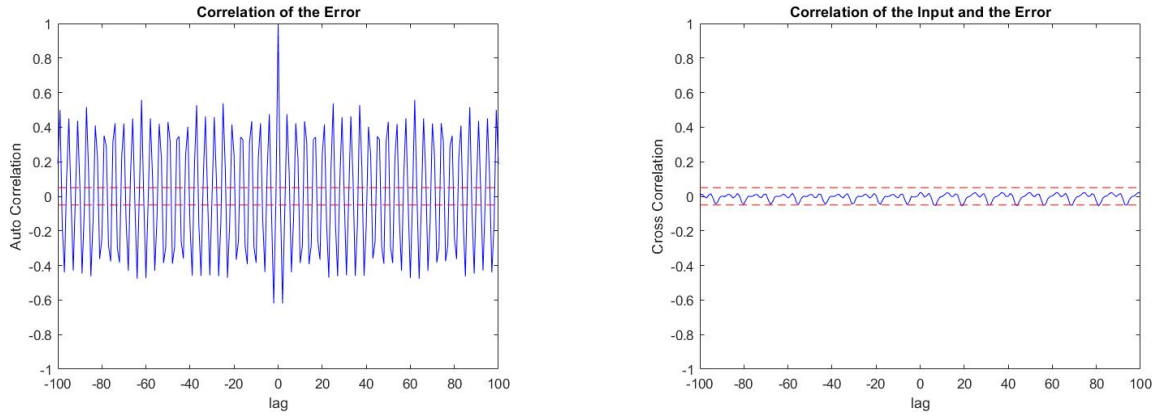

(a) (b)

Figure 10. Correlation tests of model order 6 by RLS modelling (a) autocorrelation and (b) cross-correlation

4.2 Modelling using Particle Swarm Optimization

The optimum model of the PSO algorithm was obtained by the heuristic method. Several parameters were adjusted heuristically by substituting different values of the number of particle swarm, number of iterations, inertia weight, acceleration coefficient, and model order. Firstly, the tuning process was initiated by adjusting one of the parameters at one time while the other parameters were set as constant. Then, other parameters were tuned until the optimum model of the PSO algorithm was acquired. Table 3 contains the initial PSO parameters. The optimal model order was found to be model order 2, with mean squared errors of 1.174110^{-5} and 1.067210^{-5} for training and testing data, respectively. Figure 11 represents the relationship between the mean squared error and the number of iterations. Figure 12 and Figure 13 show the actual and predicted outputs of the 30° gradient flexible plate system in the time and frequency domains. Based on Figure 12 and 13, it was demonstrated that the developed model could imitate the actual output. Figure 14 demonstrates the relatively low difference between real and estimated outputs, showing PSO's reliability in system modelling estimation.

Table 3. Parameter of the optimum model by PSO modelling

Parameter	Value
Number of particle swarm	700
Number of iterations	500
Inertia weight, ω	0.7
Acceleration coefficient, C_1 and C_2	2.0
Model order	2
MSE for training data	1.1741×10^{-5}
MSE for testing data	1.0672×10^{-5}

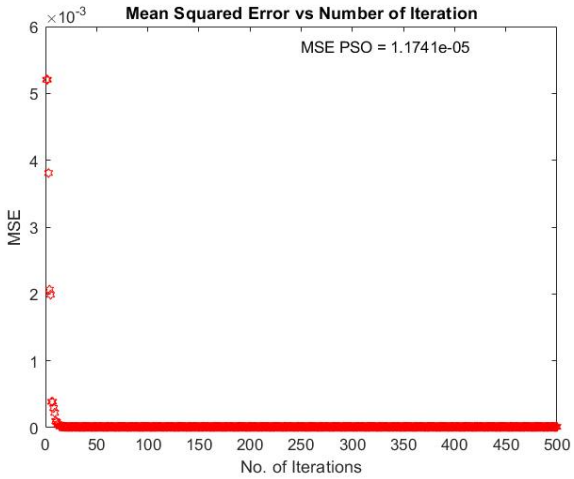

Figure 11. Mean squared error versus number of iterations by PSO modelling

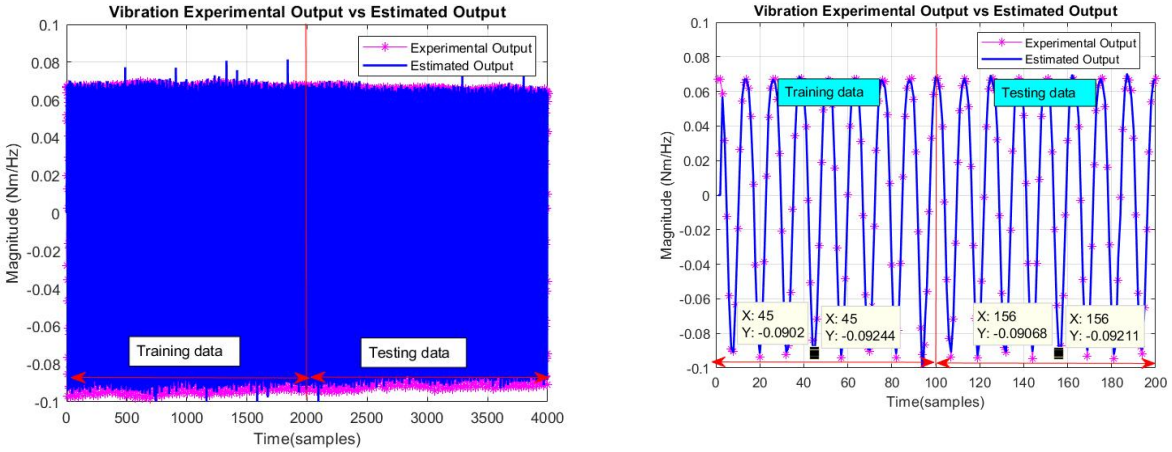

(a) (b)

Figure 12. Actual and prediction outputs of the system by PSO modelling in the time domain (a) estimated output for 4000 sample datasets and (b) an enlarged view of 200 sample datasets

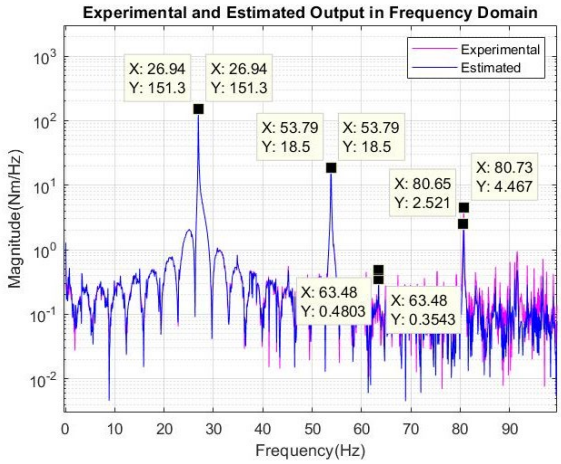

Figure 13. Actual and prediction outputs of the system by PSO modelling in the frequency domain

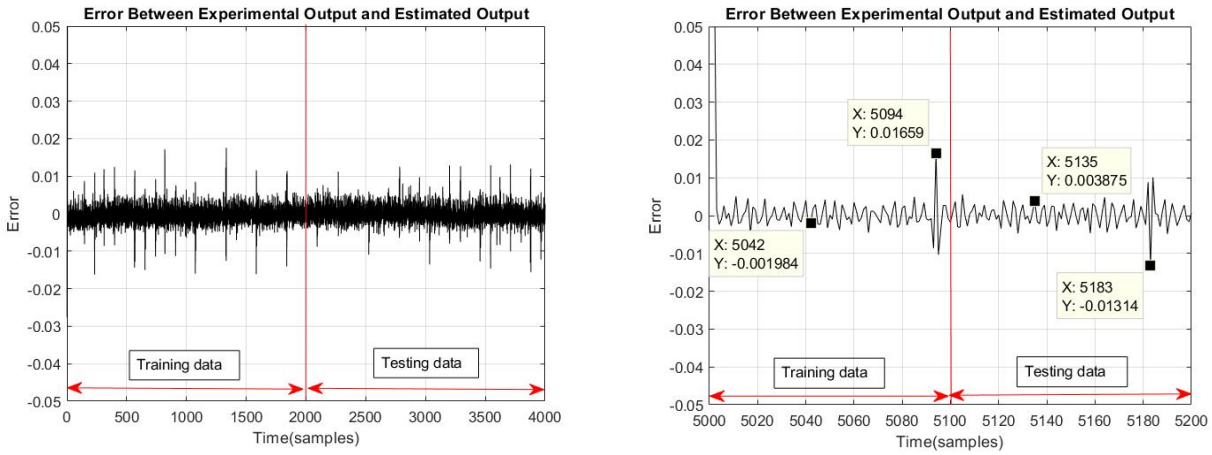

(a) (b)

Figure 14. Error between actual and estimated output by PSO modelling (a) sample for 4000 datasets and (b) an enlarged view of 200 datasets

The pole-zero diagram and correlation test are shown in Figure 11 and Figure 12, respectively. Based on the pole-zero diagram, the developed model by the PSO algorithm was stable as all the transfer function poles were inside the unity circle. The effectiveness of the developed model by the PSO algorithm was validated using autocorrelation and cross-correlation tests. Based on both correlation tests, the developed model by PSO was found to be biased as the autocorrelation did not meet the confidence level of 95%. The transfer function of the 30° gradient flexible plate system based on PSO modelling was expressed in Eq. (24).

$$H(z)_{PSO} = \frac{0.347z^{-1} - 0.0017z^{-2}}{1 - 1.414z^{-1} + 0.9938z^{-2}} \tag{24}$$

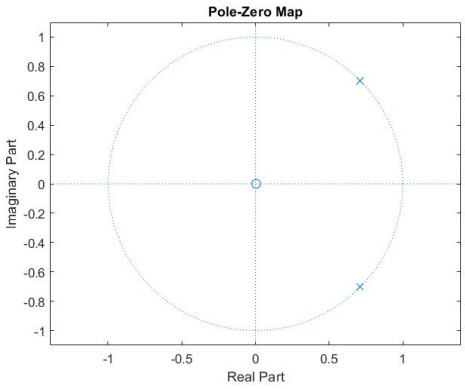

Figure 15. Pole-zero diagram system of model order 2 by PSO modelling

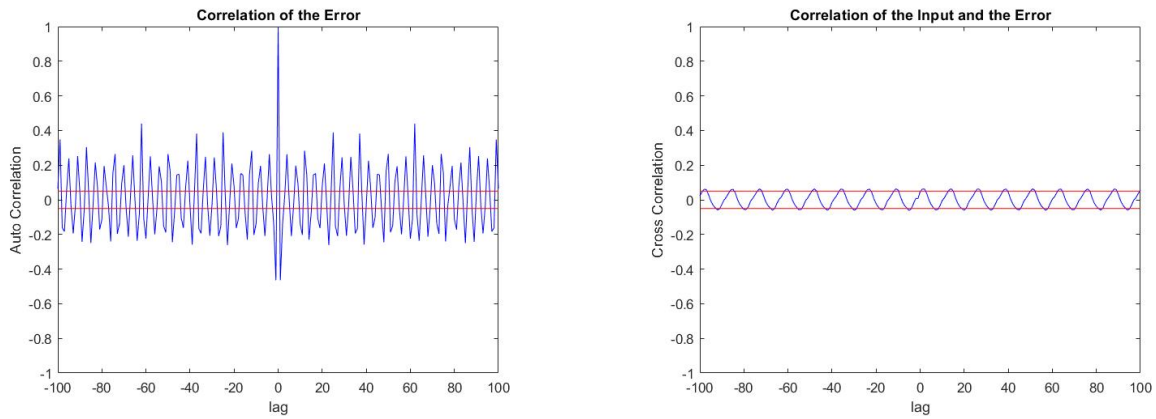

(a) (b)

Figure 16. Correlation tests of model order 2 by PSO modelling (a) autocorrelation (b) cross-correlation

The study demonstrates that when a model order of 2 is utilized, the developed mathematical model of the designated flexible plate, represented by the transfer function expressed in Eq. (24), produces a minimal MSE value. This implies

that the generated data from the mathematical model can be reasonably close to the original data. Additionally, the result of the pole-zero diagram shows that the model is stable. System stability is an essential performance criterion for a control system that must be taken into consideration. Furthermore, even though the correlation test was shown to be biased, the model can still be accepted because this biasness shows that the model is either generally applicable or tailored for certain contexts. It can be concluded that the mathematical model that was developed by PSO can represent the physical structure of the gradient flexible plate.

4.3 Modelling using Cuckoo Search

The heuristic method was also used to find the optimum model of the CS algorithm. Several parameters were heuristically changed by substituting different values for the number of nests, iterations, switch probability, lower and upper boundaries, and model order. To begin, the tuning process started by altering one of the parameters at a time while leaving the others constant. Then, various parameters were tweaked until the optimum CS algorithm model was obtained. Table 4 shows the initial settings of CS. The optimum model order was found to be model order 4, with MSE of 1.292310^{-5} and 8.191810^{-5} for training and testing data, respectively. Figure 17 depicts the relationship between the mean squared error and the number of iterations. Figure 18 and Figure 19 show the actual and predicted outputs of the 30° gradient flexible plate system in the time and frequency domains. Based on Figure 18 and 19, it was demonstrated that the developed model could mimic the actual output. Figure 20 demonstrates the significantly low difference between actual and estimated outputs, indicating CS capability in system modelling estimation.

Table 4. Parameter of the optimum model by CS modelling

Parameter	Value
Number of nests	16
Number of iterations	2500
Switch probability	0.01
Lower and upper boundary	[-1,1]
Model order	4
MSE for training data	1.2923×10^{-5}
MSE for testing data	8.1918×10^{-6}

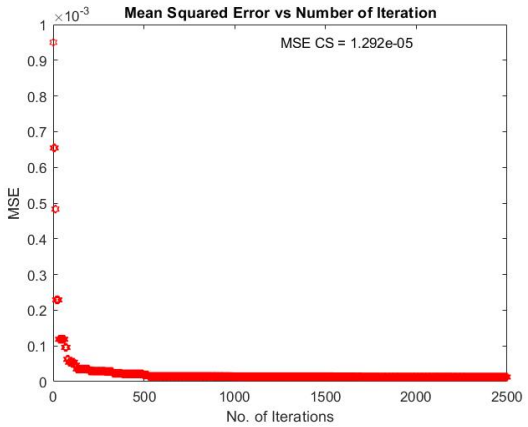

Figure 17. Mean squared error versus number of iterations by CS modelling

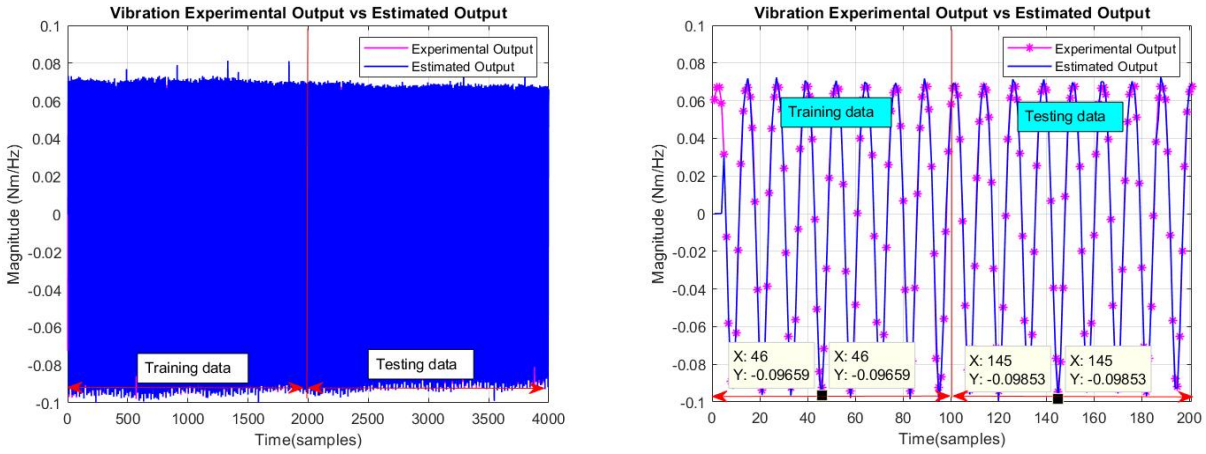

(a) (b)

Figure 18. Actual and prediction outputs of the system by CS modelling in the time domain (a) estimated output for 4000 sample datasets (b) enlarged view of 200 sample datasets

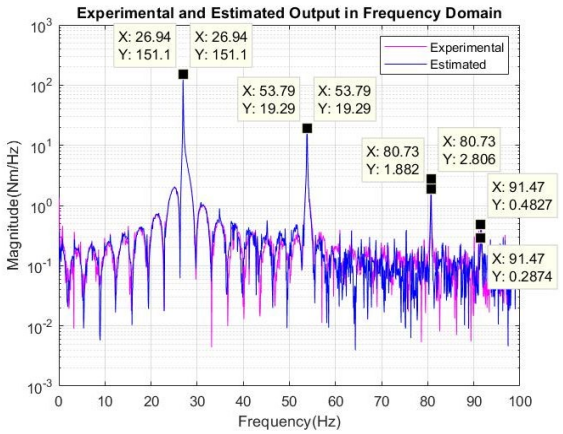

Figure 19. Actual and prediction outputs of the system by CS modelling in the frequency domain

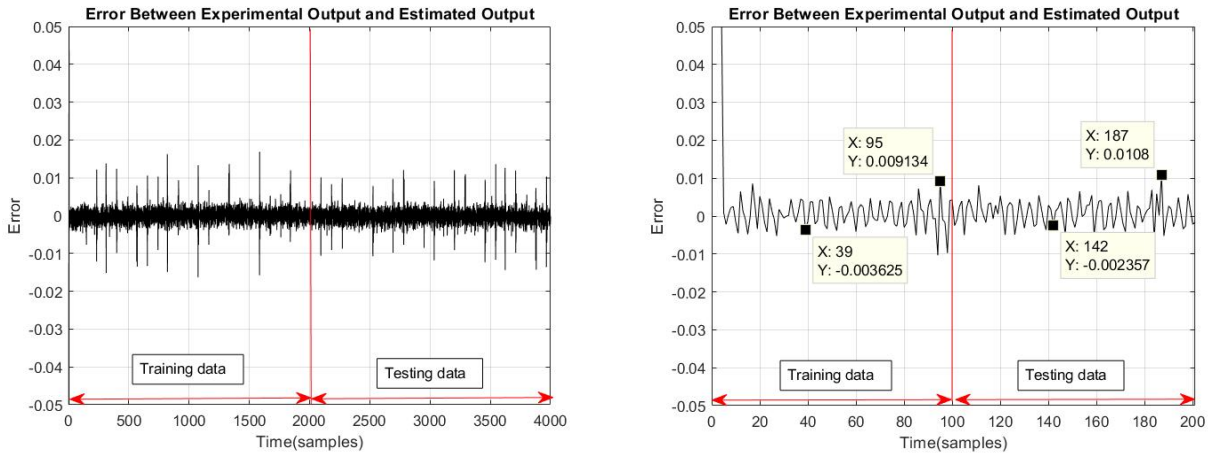

(a) (b)

Figure 20. Error between actual and estimated output by CS modelling (a) sample for 4000 datasets and (b) an enlarged view of 200 datasets

Figure 21 and 22 show the pole-zero diagram and the correlation test, respectively. According to the pole-zero diagram, the produced model by the CS algorithm was stable because all of the transfer function poles were inside the unity circle. The effectiveness of the developed model by the CS algorithm was confirmed using autocorrelation and cross-correlation tests. Based on both correlation tests, CS's developed model was confirmed to be unbiased, as the autocorrelation reaches the confidence threshold of 95%. Equation (25) represents the transfer function of a 30° gradient flexible plate system based on CS modelling.

$$H(z)_{PSO} = \frac{0.419z^{-1} + 0.005415z^{-2} + 0.6701z^{-3} - 0.2692z^{-4}}{1 - 0.3435z^{-1} + 0.2047z^{-2} - 0.05312z^{-3} + 0.7253z^{-4}} \quad (25)$$

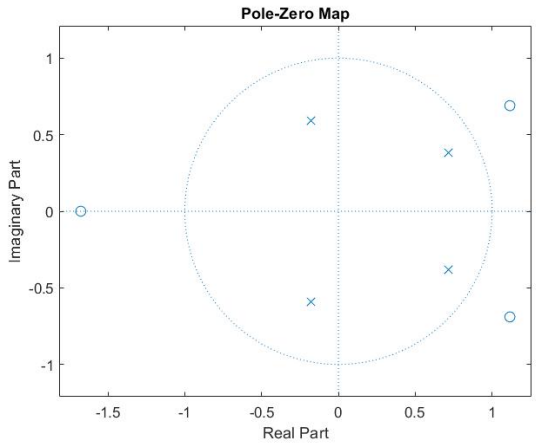

Figure 21. Pole-zero diagram system of model order 4 by CS modelling

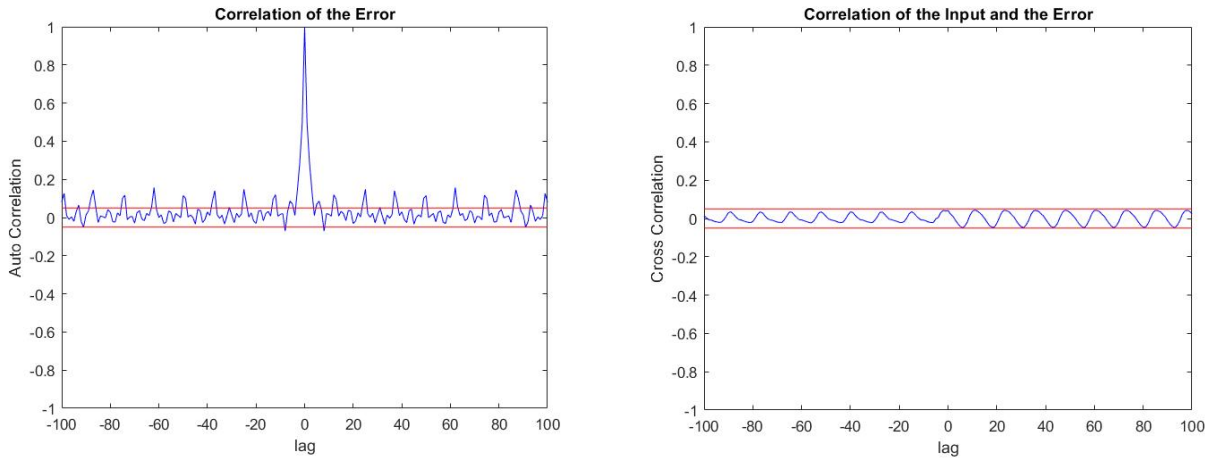

(a) (b)

Figure 22. Correlation tests of model order 4 by CS modelling (a) autocorrelation (b) cross-correlation

The study reveals that the constructed mathematical model of the designated flexible plate, represented by the transfer function indicated in Eq. (25), generates the lowest MSE value when a model order of 4 is utilized. This suggests that the data obtained by the mathematical model may be rather close to the data generated beforehand. The pole-zero diagram's outcome further demonstrates that the model is stable. An important performance criterion for a control system that must be taken into account is system stability. The model also shows unbias in the correlation test, which complies with Eq. (21) and (22). This indicates that it is widely applicable to various settings. It can be claimed that the physical characteristics of gradient flexible plate are accurately captured by the mathematical model that was produced by CS.

4.4 Comparative Assessment and Evaluation

The performance of the developed model was compared and reviewed based on mean squared error, correlation tests, and pole-zero diagram stability. The accuracy of the system is determined by fulfilling all of the requirements of each validation. Table 5 summarises the modelling performance for a flexible plate system with a 30° gradient. According to Table 5, the lowest PSO modelling MSE value for training data was 1.174110^{-5}, while the lowest MSE value for CS modelling testing data was 8.191810^{-6}. From these observations, both intelligent algorithms PSO and CS outperformed the traditional RLS.

In terms of a good correlation test, the obtained result must be within a 95 percent confidence level. According to Table 5, only the CS algorithm indicates unbiased owing to the dynamic system being within 95 percent confidence level. RLS and PSO, on the other hand, failed to satisfy the criterion to obtain a 95 percent confidence level. Therefore, both the RLS and the PSO dynamic systems were identified as biased. In this case, the CS model has proven to be superior to RLS and PSO since it has a low MSE value and signifies unbiasedness.

Aside from that, the stability of the pole-zero diagram is an indicator for considering the optimum model representing the system by taking the placement poles in the pole-zero diagram into account. The model was considered stable if the poles were positioned inside the unit circle. Table 3 reveals that all models developed were stable, as determined by the observation that all poles plotted were within the unit circle area.

Based on the results of the assessments, it can be concluded that the evolutionary algorithm was significantly more reliable than the conventional algorithms, with the CS algorithm modelling being the best model for accurately capturing the actual 30° gradient flexible plate structure. As previously discussed, all of the models can be used to represent the gradient flexible plate system. However, the model derived from the CS algorithm meets all of the criteria, making it the most suitable model for controller development. Hence, the CS model transfer function will be used for controller development to suppress undesirable vibration on the 30° gradient flexible plate system.

Table 5. Summary of performance modelling 30° gradient flexible plate system

Model	Model order	MSE in training data	MSE in testing data	Stability	Correlation test
RLS	6	6.6453×10^{-4}	7.4162×10^{-5}	Stable	Biased
PSO	2	1.1741×10^{-5}	1.0672×10^{-5}	Stable	Biased
CS	4	1.2923×10^{-5}	8.1918×10^{-6}	Stable	Unbiased

5.0 CONCLUSIONS

This paper discussed the development of the dynamic model for 30° gradient flexible plate structure using the system identification (SI) technique. The models were estimated using evolutionary algorithms PSO and CS algorithm based on the structure of ARX model. For comparison purposes, the conventional method, RLS, was also estimated. The models obtained were validated by three methods: MSE, pole-zero stability, and correlation tests. The optimum model that met

all of the criteria was selected to be the ideal model to represent the 30° gradient flexible plate structure. Based on the findings, model order 4 by the CS algorithm was chosen since it had the lowest MSE value of 8.191810^{-6}, resulting in an 89 % improvement over RLS. In addition, when compared to RLS and PSO, the CS algorithm demonstrated great stability and good correlation tests. This correlation test is critical to indicate the efficacy level of the established model. To conclude, the ideal model obtained from CS can be applied in control development to suppress vibration on the 30° gradient flexible plate system.

6.0 ACKNOWLEDGEMENT

The authors would like to express their gratitude to the Minister of Higher Education Malaysia (MOHE) and Universiti Malaysia Sarawak (UNIMAS) for funding and providing facilities to conduct this study.

7.0 REFERENCES

[1] Y. Bao, B. Wang, Z. He, R. Kang, and J. Guo, "Recent progress in flexible supporting technology for aerospace thin-walled parts: A review," Chinese Journal of Aeronautics, vol. 35, no. 3, pp. 10-26, 2022.

[2] W. Zhaohui, D. Ji-wang, Z. Minghua, and F. Xiumin, "Survey on flexible shipbuilding technologies for curved ship-blocks," Procedia Engineering, vol. 174, pp. 800-807, 2017.

[3] K. Draganová, K. Semrád, M. Spodniak, and M. Cúttová, "Innovative analysis of the physical-mechanical properties of airport conveyor belts," Transportation Research Procedia, vol. 51, pp. 20–27, 2020.

[4] S. Julai, M. O. Tokhi, M. Mohamad, and I. Abd. Latiff, "Control of a flexible plate structure using particle swarm optimization," In 2009 IEEE Congress on Evolutionary Computation, 2009, pp. 3183-3190.

[5] A.R.Tavakolpour, I. Z. M. Darus, M. O. Tokhi, and M. Mailah, "Genetic algorithm-based identification of transfer function parameters for a rectangular flexible plate system," Engineering Applications of Artificial Intelligence, vol. 23, no. 8, pp.1388-1397, 2010.

[6] M. J. Mohammed, M. K. Ahmed, and B. A. Abbas, "Modeling and control of horizontal flexible plate using PID-CS controller," *Journal of Mechanical Engineering Research and Developments*, vol. 42, no. 4, pp. 138–142, 2019.

[7] M. Marinaki, Y. Marinakis, and G. E. Stavroulakis, "Vibration control of beams with piezoelectric sensors and actuators using particle swarm optimization," *Expert Systems With Applications*, vol. 38, no. 6, pp. 6872–6883, 2011.

[8] S. Khooshechin, F. Mansourzadeh, M. Imani, J. Safdari and M. H. Mallah, "Optimization of flexible square cascade for high separation of stable isotopes using enhanced PSO algorithm," *Progress in Nuclear Energy*, vol. 140, p. 103922, 2021.

[9] D. Negri, F. K. Fiorentin, and J. M. C. Filho, "A model updating method for plate elements using particle swarm optimization (PSO), modeling the boundary flexibility, including uncertainties on material and dimensional properties," *Latin American Journal of Solids and Structures*, vol. 15, no. 10, pp.1-18, 2018.

[10] K. Belhadj, N. B. Guedria, A. Helali, and C. Bouraoui, "A two-stage approach to solve structural damage detection problem in plate structures," in *Advances in Materials, Mechanics and Manufacturing II. A3M 2021. Lecture Notes in Mechanical Engineering*, M. Ben Amar, A. Bouguecha, E. Ghorbel, A. El Mahi, F. Chaari, and M. Haddar, Eds. Cham: Springer, 2022, pp. pp. 63 -72.

[11] J. Wang, M. Liu, W. Liao, K. Yun, Y. Tan, and Z. Zhang, "Spline interpolation method based on arc length parameterization and its application in stress field interpolation for flexible plates," in *IEEE Access*, vol. 9, pp. 35879-35887, 2021.

[12] S. Julai, M. O. Tokhi, M. Mohamad, and I. A. Latiff, "Active vibration control of a flexible plate structure using particle swarm optimization," In 2010 IEEE 9th International Conference on Cyberntic Intelligent Systems, 2010, pp. 1-6.

[13] A Jamali, I.Z.M. Darus, "Intelligent evolutionary controller for flexible robotic arm", *Journal of Physics: Conference Series* vol. 1500, no. 1, p. 012020, 2020.

[14] X. S. Yang, S. Deb, "Cuckoo search: recent advances and applications," *Neural Computing & Applications,* vol. 24, pp. 169–174, 2014.

[15] H. Tran-Ngoc, S. Khatir, G. D. Roeck, T. Bui-Tien, and M. A. Wahab, "An efficient artificial neural network for damage detection in bridges and beam-like structures by improving training parameters using cuckoo search algorithm," *Engineering Structures,* vol. 199, pp.1-16, 2019.

[16] A. A. S. N. Sukri, S. S. Z. Nazri, M. S. Hadi, A. Jamali, H. M. Yatim and I. Z. M. Darus, "Hub angle control for a single-link flexible manipulator based on Cuckoo Search algorithm," In 2021 IEEE 7th International Conference on Smart Instrumentation, Measurement and Applications (ICSIMA), pp. 162-167, 2021.

[17] A. A. Al-Khafaji and I. Z. M. Darus, "Controller optimization using cuckoo search algorithm of a flexible single-link manipulator," In *1st International Conference on System Informatics, Modelling and Simulation*, pp. 39-44, 2014.

[18] H. J. Xu, J. K. Liu, and Z. R. Lu, "Structural damage identification based on cuckoo search algorithm," *Advances in Structural Engineering,* vol. 19, no. 5, pp. 849-859, 2016.

[19] I. Z. M. Darus, A. A. M. Al-Khafaji, and M. F. Jamid, "Neuro modelling of flexible plate structure rig for development of active vibration control algorithm," In *Asia International Conference on Modelling & Simulation,* pp. 396-401, 2010.

[20] D. Freitas, L. G. Lopes, and F. Morgado-Dias, "Particle swarm optimization: A historical review up to the current developments," *Entropy*, vol. 22, no. 3, pp. 1–36, 2020.

[21] A. A. M. Al-Khafaji, I. Z. M. Darus, and M. F. Jamid, "ANFIS modelling of flexible plate structure," In 2010 1st International Conference on Energy, Power and Control, vol. 6, no. 1, pp. 78–82, 2010.